9-Substituted Triptycene as a Probe for the Study of Internal Rotation around a C–PH Bond in the Solid State: A Single Crystal EPR Study at Variable Temperature†

ARTICLE *in* THE JOURNAL OF PHYSICAL CHEMISTRY · JUNE 1996

Impact Factor: 2.78 · DOI: 10.1021/jp960836h

4 AUTHORS, INCLUDING:

Geetha Ramakrishnan
Sathyabama University
20 PUBLICATIONS **68** CITATIONS
SEE PROFILE

Michel Geoffroy
University of Geneva
207 PUBLICATIONS **2,081** CITATIONS
SEE PROFILE

9-Substituted Triptycene as a Probe for the Study of Internal Rotation around a C−PH Bond in the Solid State: A Single Crystal EPR Study at Variable Temperature†

Geetha Ramakrishnan,‡ Abdelaziz Jouaiti,‡ Michel Geoffroy,*,‡ and Gérald Bernardinelli§

Department of Physical Chemistry, 30 Quai Ernest Ansermet, University of Geneva, 1211 Geneva, Switzerland, and Laboratory of X-ray Crystallography, 24 Quai Ernest Ansermet, University of Geneva, 1211 Geneva, Switzerland

Received: March 19, 1996⊗

To measure the rotation barrier around an $R_3C-{}^{\bullet}PH$ bond in the solid state, 9-phosphinotriptycene[50] **2** has been synthesized and its crystal structure has been determined. It is shown, by EPR, that the radiogenic radical **3**, which results from a homolytic scission of a P−H bond, can indeed be trapped in the crystal matrix. Its **g**-tensor together with its ^{31}P and ^{1}H hyperfine coupling have been measured at 300 and 77 K. These tensors show that free rotation around the C−P bond occurs at room temperature but is blocked at liquid nitrogen temperature. The temperature dependence of the EPR spectra has been analyzed using the density matrix formalism and has led to a rotation barrier of about 2.5 kcal·mol^{-1} . This result and the various hyperfine couplings have been compared with the values predicted by ab initio methods for two isolated model radicals: the *tert*-butylphosphinyl radical **4** and the barrelenophosphinyl radical **5**.

Introduction

Restricted rotation about a single bond is invoked in a large variety of chemical processes and has been successfully investigated by numerous spectroscopic methods[1,2] (NMR, microwave spectroscopy, IR, Raman). The number of available techniques becomes, however, drastically more limited when one of the two atoms that form the single bond bears an unpaired electron. The knowledge of the height of the potential barrier to rotation about such an $A-B^{\bullet}$ bond is essential for understanding mechanisms involving radical intermediates. Whereas EPR/ENDOR measurements in solution[3−8] have been widely used to study conformational flips, diffusional rotations, and hindered rotations of groups exhibiting couplings with nuclei located β to the radical center, the number of studies dealing with internal rotation of a radical moiety centered on a heteroatom is considerably smaller. This is mainly due to the fact that the systems appropriate to such investigations are difficult to find; the lifetime of these species is often very short, and frequently, the EPR spectrum reveals the presence of secondary species, which preclude any variable temperature study. A better approach is to study the hindered rotation after trapping the radical inside a diamagnetic crystal matrix. Curiously, this method has not been considerably explored[9] and the research groups active in this field have mainly concentrated either on the rotation of a $^{\bullet}CH_2$ (or a $^{\bullet}CF_2$)[10−20] α to $C(O)O^-$ or on the rotation of a methyl group α to a radical center.

In the present study our purpose is to study the internal rotation around the $C-P^{\bullet}$ bond in the case of the simplest organophosphorus radical **1**. To generate this radical and to measure the height of the potential barrier to rotation, we need a precursor that fulfills the following criteria: (i) the R_3C group must be bulky and rigid in such a way that the rotation around the C−P bond is the only motion present in the sample; (ii) the carbon atom of the R_3C group must be perfectly tetrahedral, and no steric interaction between this group and the PH bond can hinder the rotation around the P−C bond; (iii) the R_3C group must not be likely to produce any radical that could mask the EPR spectrum, and the phosphine group must easily undergo a specific homolytic scission. All these conditions led us to synthesize the new phosphine **2** where the triptycyl group—probably less sensitive to ionizing radiation—is bound, in position 9, to the PH_2 moiety, which is expected to easily give rise to the radiogenic phosphinyl radical **3**. A similar approach has already been followed for the study of internal rotation in stable diamagnetic compounds, and NMR spectroscopy has yielded valuable information about rotation isomerism for 9-substituted triptycenes.[21−26]

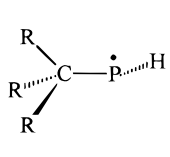

1

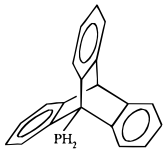

2

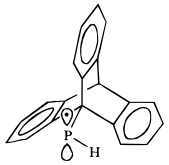

3

In the present study, after determination of the various EPR tensors at low temperature (when the motion is blocked) and at high temperature (when the motion is free), the reliability of the system was checked by comparing the orientation of the eigenvectors with that of the bond directions obtained from the crystal structure. The temperature dependence of the spectrum, analyzed by using the density matrix formalism, then led to an estimation of the energy barrier to rotation about the C−P bond. This barrier, obtained for a radical trapped in a crystal environment, was then compared to that of an isolated model radical as predicted by ab initio calculations.

Experimental Section

Irradiation and Crystal Mounting. After indexation of its faces, a single crystal of **2** was sealed in an evacuated glass tube (10^{-5} Torr) and exposed for 2 h, at room temperature, to the emission of a Philips X-ray generator (tungsten anticathode, 30 kV, 30 mA). The irradiated crystal was coated with an inert adhesive medium to prevent the decay of the trapped radicals, which was probably caused by the effect of oxygen. Then the

† Dedicated to Professor Edwin A. C. Lucken on the occassion of his 65th birthday.

‡ Department of Physical Chemistry.

§ Laboratory of X-ray Crystallography.

⊗ Abstract published in *Advance ACS Abstracts,* May 15, 1996.

S0022-3654(96)00836-2 CCC: $12.00

crystal was glued on a small brass cube and studied by EPR. The crystal showed neither the {100} nor the {001} face (see below), so the brass cube was truncated in such a way that the crystallographic *c*-axis was aligned along the *Z*-axis of the EPR reference frame. The *X*- and *Y*-axes were coincident with the *a**- and *b*-axes, respectively.

Single Crystal EPR Study. The EPR spectra were recorded on a Bruker-200D spectrometer (X-band, 100 kHz field modulation) equipped with a VT 1100 variable temperature controller. The angular dependence of the signals was studied by rotating the crystal, glued on the small cube, around three perpendicular axes. The spectra were recorded in steps of 10° at 300 K. The same type of experiment was also performed at 77 K using a finger Dewar. The various EPR tensors were determined using an optimization program[27] that calculates the position of the resonance signals using second-order perturbation theory.[28] The Hamiltonian took the electronic and nuclear Zeeman effects into account as well as the hyperfine couplings with a ^{31}P and a ^{1}H nucleus. The resulting tensors were checked by using a program that directly diagonalizes the Hamiltonian and calculates the resulting line positions. The temperature dependence of the spectra was analyzed by determining, for each temperature, the rotational correlation time τ_c that leads to the best simulation of the experimental spectrum.

EPR Spectra Simulation. The spectrum has been simulated by calculating $I(\omega) = \mathrm{Re}\{\langle S^+(\omega)\rangle\} = \mathrm{Tr}(\boldsymbol{\rho} S^+) = \mathrm{Tr}(\boldsymbol{\rho}^{-+})$. The 12 × 12 matrix **L**, for an exchange among three sites *a*, *b*, and *c*, is defined in the Liouville space as

$$\mathbf{L} = \begin{bmatrix} (i\mathbf{H}_a - 1/T_2) & 0 & 0 \\ 0 & (i\mathbf{H}_b - 1/T_2) & 0 \\ 0 & 0 & (i\mathbf{H}_c - 1/T_2) \end{bmatrix} + \begin{bmatrix} -(k_{ab} + k_{ac})\mathbf{1} & k_{ab}\mathbf{1} & k_{ac}\mathbf{1} \\ k_{ba}\mathbf{1} & -(k_{ba} + k_{bc})\mathbf{1} & k_{bc}\mathbf{1} \\ k_{ca}\mathbf{1} & k_{cb}\mathbf{1} & -(k_{ca} + k_{cb})\mathbf{1} \end{bmatrix}$$

k_{ij} ($=\tau_{ij}^{-1}$) is the exchange rate between sites *i* and *j*.[11] **1** is the 4 × 4 unit matrix. $\mathbf{H}_k$ is a 4 × 4 diagonal matrix whose H_{ii} elements represent the allowed transitions. After separation of the terms in ω, **L** is written as $\mathbf{L} = [\boldsymbol{\Omega} - i\omega\mathbf{1}]$ (in this expression **1** is a 12 × 12 unit matrix) and $\boldsymbol{\Omega}$ is diagonalized: $\boldsymbol{\Omega} = \mathbf{U}^{-1}\boldsymbol{\Lambda}\mathbf{U}$. For each value of ω the intensity is obtained by summing the 12 elements of the vector $\boldsymbol{\rho}^{-+}$:

$$\boldsymbol{\rho}^{-+} = iI_0 \cdot [\mathbf{U}^{-1}\boldsymbol{\Lambda}\mathbf{U} - i\omega \cdot \mathbf{1}]^{-1}\boldsymbol{\nu}$$

where $\boldsymbol{\nu}$ is a column vector whose 12 elements are equal to 1. The values of $\mathbf{H}_k$ correspond to the difference of two diagonal terms of the Hamiltonian, expressed in Hilbert space. They are obtained, for each site, from the **g** and hyperfine tensors **T** determined from the low-temperature EPR study. Similarly, with the method proposed by Benetis et al.[12,13] at temperature *T* and for an orientation **v** of the magnetic field, the spectrum is generated from the three pseudoisotropic spectra[8] observed, at 77K, for this orientation. Each of these spectra is associated with a site *k* and is characterized by an effective *g* value and a hyperfine interaction respectively given by $g_k = [\mathbf{v}' \cdot \mathbf{g}_k \cdot \mathbf{g}_k \cdot \mathbf{v}]^{-1/2}$ and $A_k = [\mathbf{v}' \cdot \mathbf{g}_k \cdot \mathbf{T}_k \cdot \mathbf{T}_k \cdot \mathbf{g}_k \cdot \mathbf{v})/g^2]^{-1/2}$ where $\mathbf{v}'$ and **v** are the array and column vectors whose elements are the direction cosines of the magnetic field.

Ab Initio Calculations. The calculations were carried out on a Silicon Graphics computer (IRIS 4D) using the Gaussian 92 program.[29,30] All the results for the *tert*-butylphosphinyl radical **4** have been obtained at the MP2 level by using the UHF method and the 6-31G* basis set. For the barrelenophosphinyl radical **5**, the larger size of the radical compelled us to use the 3-21G* basis set at the SCF level**.** Spin densities and hyperfine couplings have been calculated after annihilation of spin contamination.

Crystal Data. $C_{20}H_{15}P$, $M_r = 286$, $\mu = 1.585$ mm^{-1}, $F(000) = 900$, $d_x = 1.33$ Mg·m^{-3}, trigonal, *R*3*c* (hexagonal axes), $Z = 6$, $a = 12.0185(8)$, $c = 17.215(1)$ Å, $V = 2153.5(3)$ Å^3 from 21 reflections ($43° < 2\theta < 79°$). Colorless trigonal prism (obtained by slow evaporation from a CH_2Cl_2 / EtOH mixture) of average dimensions 0.18 mm × 0.18 mm × 0.18 mm with faces {$\bar{1}02$} (well developed), {$1\bar{1}2$}, {012} was mounted in a capillary to prevent decomposition.

Cell dimensions and intensities were measured at 200 K on an Enraf−Nonius CAD-4 diffractometer with graphite-monochromated Cu Kα radiation ($\lambda = 1.5418$ Å), $\omega - 2\theta$ scans, scan width of $1.6° + 0.14 \tan\theta$, and scan speed 0.02−0.14 deg/s. Two reflection references measured every 45 min show a variation of less than $2.5\sigma(I)$. $0 < h < 11$; $0 < k < 11$; $-19 < l < 19$. A quantity of 709 unique reflections were measured of which 666 were observable ($|F_o| > 4\sigma|F_o|$), and $\sum(\sigma|F_o|)/\sum(\sigma|F_o|) = 0.023$. Data were corrected for Lorentz and polarization effects and for absorption[31] ($A^*_{min} = 1.474$, $A^*_{max} = 1.891$). The structure was solved by direct methods using MULTAN 87,[32] and all other calculations used the XTAL[33] system and ORTEP[34] programs. Atomic scattering factors and anomalous dispersion terms were taken from ref 35.

Crystal Structure Determination for 2. The molecules are located on 3-fold axes with P, C(1), and C(8) atoms in special positions 6a. Refinement on the structure in the space group *R*3*c* (*R* ≈ 13%) leads to a chirality/polarity parameter[36,37] converging to $x = 0.37(32)$ and shows a residual electron density of about 3 e Å^{-3} on the 3-fold axis at 1.9 Å of the C(8) atom. Moreover, the displacement parameters of the carbon atoms are unusually elongated along the *z* direction or nonpositively defined. These results suggest that the structure is not only twinned but disordered as well. Refinements in the centrosymmetric space group $R\bar{3}c$, with a 50/50 disordered model or the corresponding 2-fold related half asymmetric unit, show no residual peak on the 3-fold axis but lead to high (∼15%) *R* values. Finally, the refinement of a partially disordered model in the space group *R*3*c* shows that the disorder consists of an inversion of the molecule approximately maintaining the position of the triptycene skeleton and mainly affecting the phosphorus atom. The refinement of such a model fixing the sum of the occupations of the P(1) and P(2) sites to 1 shows a disorder ratio of 73.4(5)/26.6(5)%. The final displacement parameters show that a splitting of the atomic sites of the carbon atoms was not necessary. Furthermore, the final value of the chirality/polarity parameter converges to $x = 0.35(8)$, confirming that the crystal is partially twinned in a ratio of 65/35%. The structure was refined by full-matrix least-squares, based on $|F|$, using weights of $1/\sigma^2(|F_o|)$, and the polar origin was defined as a shift-limiting restraint: $z(P(2)) = -z(P(1))$. All coordinates and isotropic displacement parameters of the aromatic hydrogen atoms have been refined. The remaining hydrogen linked to the phosphorus and C(8) atoms have been observed and contributed to the $|F_c|$ calculations but have not been refined. Isotropic extinction was applied: $g = 0.21(2) \times 10^{-4}$. The final values $R = 0.037$, $\omega R = 0.032$, and $S = 4.53$ are obtained for 85 variables and 666 contributing reflections. The mean and maximum shift/error on the last cycle was 0.0064 and 0.046, respectively. The final difference electron density map showed a maximum of 0.17 and a minimum of −0.10 e Å^{-3}. It should be noted that the *coordinates* of the atoms in the structure are centrosymmetric, as can be shown by the MISSYM program.[38]

TABLE 1: Atomic Coordinates, Equivalent Isotropic Displacement Parameters (Å²), and Population Paramaters (If ≠ 1) with Estimated Standard Deviations in parentheses for 9-Phosphinotriptycene 2[a]

	x/a	*y/b*	*z/c*	U_{eq}	PP
P(1)	0	0	0.0632(6)	0.043(1)	0.734(5)
P(2)	0	0	−0.0632(6)	0.058(4)	0.266(5)
C(1)	0	0	0.1736(6)	0.041(4)	
C(2)	0.1176(5)	0.1166(5)	0.2076(9)	0.032(3)	
C(3)	0.2179(6)	0.2166(7)	0.167(1)	0.044(3)	
C(4)	0.3177(6)	0.3146(7)	0.209(1)	0.050(4)	
C(5)	0.3176(9)	0.3159(7)	0.290(1)	0.058(5)	
C(6)	0.2163(6)	0.2149(7)	0.329(1)	0.046(4)	
C(7)	0.1176(5)	0.1169(5)	0.288(1)	0.041(3)	
C(8)	0	0	0.3246(6)	0.034(3)	
H(3)	0.219(5)	0.208(5)	0.108(3)	0.04(2)	
H(4)	0.377(6)	0.376(6)	0.173(4)	0.06(2)	
H(5)	0.394(5)	0.386(6)	0.311(4)	0.05(2)	
H(6)	0.226(6)	0.218(6)	0.386(3)	0.06(2)	
H(8)	0	0	0.3802	0.040	0.7
H(8a)	0	0	0.1185	0.040	0.3
H(01)	0.0082	0.0743	0.0547	0.050	0.5
H(02)	0.1058	0.0946	−0.0442	0.050	0.2

[a] U_{eq} is the average of eigenvalues of *U*.

However, our results clearly and definitely indicate that the *structure* is noncentrosymmetric and disordered and the crystal is twinned by inversion.

Synthesis of 9-Phosphinotriptycene 2. NMR spectra were recorded on a Bruker AC-200F (^{1}H, 200 MHz; ^{31}P, 81 MHz) spectrometer. External H_3PO_4 was used as reference for ^{31}P NMR. A quantity of 4 mL (6.4 mmol) of *n*-BuLi (1.6 M in hexane) was slowly added, at −80 °C, to a solution containing 2 g (6 mmol) of 1-bromotriptycene[39] in 30 mL of dry THF. The mixture was left to warm to ambient temperature and was cooled again at −80 °C. A sample of 1.25 g of PCl_3 (9.1 mmol) was then added in one portion, and the solution was refluxed for 1.5 h. This cooled solution was slowly added, at 0 °C, to a suspension of 0.4 g of $LiAlH_4$ (10 mmol) in 30 mL of THF. After hydrolysis with HCl (2 N) the solution was extracted with ether and the organic phase was dried with $MgSO_4$. After evaporation to dryness the compound was purified by recrystallization from CH_2Cl_2/ C_2H_5OH. Melting point, 220−222 °C. ^{31}P{^{1}H} NMR (CD_2Cl_2) d −156 ppm. ^{1}H NMR (CD_2Cl_2) δ = 3.76 (d, 2H, J_{H-P} = 201.6 Hz), 5.48 (s, 1H), 7.08 (m, 2H), 7.44 (m, 1H), 7.58 (m, 1H) ppm.

Results

Crystal Structure. The twinning and/or disorder with interchange of the bridgehead carbon atom observed in **2** is closely related to those observed for arsatriptycene and phosphatriptycene.[40] This last compound shows a twinning through a plane with the molecules in general positions, whereas in **2** an inversion twin was observed with molecules located on 3-fold axes. The atomic coordinates for **2** are given in Table 1, and a perspective view of the molecule is shown in Figure 1. The geometrical parameters of the triptycene moiety in **2** (C(1)−C(2) = 1.524(8) Å, C(7)−C(8) = 1.541(9) Å, mean value C_{ar}−C_{ar} = 1.385 Å, C(1)−C(2)−C(7) = 112.7(7)°, C(2)−C(7)−C(8) = 113.7(7)°) are in good agreement with other triptycene derivatives.[22,41−43] All non-H atoms of the asymmetric unit are coplanar (maximum deviation of the mean plane = 0.008 Å for C(4)), and on account of the symmetry location of the molecule, no deformation occurs for the dihedral angles of the three benzene rings. The bridgehead carbon atoms show a slight deformation from ideal tetrahedral bond angles (C(2)−C(1)−C(2′) = 106.2(7)°, C(7)−C(8)−C(7′) = 104.8(7)°, C(2)−C(1)−P(1) = 112.6°). Because of the presence of the 3-fold axis,

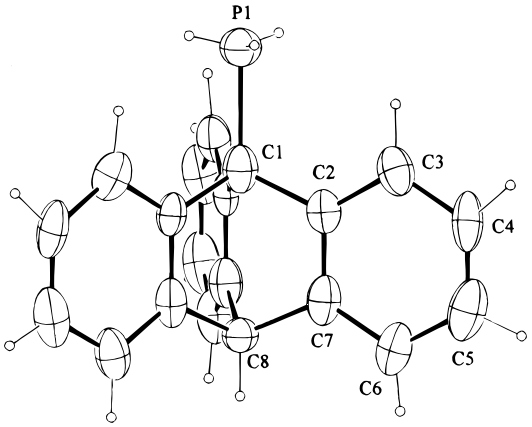

Figure 1. Perspective view of the 9-phosphinotriptycene **2** (major constituent) with atom numbering. Ellipsoids are represented with 50% probability level.

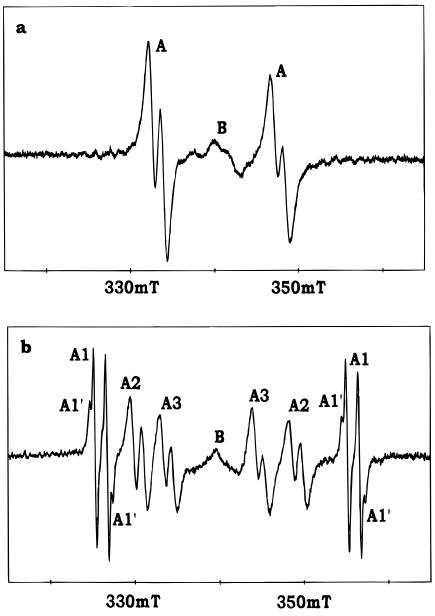

Figure 2. EPR spectra obtained with an X-irradiated single crystal of **2** (the magnetic field lies in the *a*b* plane, 20° from the *b*-axis): (a) at room temperature; (b) at 77 K.

the hydrogen atoms of the phosphine moiety are disordered. Nevertheless, the atomic sites of the H atoms bonded to the phosphorus have been observed and show staggered conformations relative to the benzene rings (H(01)−P(1)−C(1)−C(2) = −55°, H(02)−P(2)−C(8)−C(7) = 66°). The phosphorus atom is pyramidal with C−P−H bond angles of 99.8 and 105.1°, respectively, for the major and minor constituents of the disorder.

EPR Spectra. An example of an EPR spectrum recorded at room temperature with an X-irradiated single crystal of **2** is shown in Figure 2a. This spectrum**,** obtained when the magnetic field lies in the *a*b* plane 20° from the *b*-axis, is mainly due to the presence of a radical that exhibits hyperfine interaction with a ^{31}P and a ^{1}H nucleus. Besides these signals (marked A in Figure 2a) a much less intense singlet (marked B) is also detected in the central part of the spectrum. The EPR spectrum obtained for the same orientation, at 77 K, is shown in Figure 2b. Although the B signal is almost not affected by temperature, the subspectrum A is now split into three sets of signals marked A1, A2, and A3. Each set is still characterized by a coupling to a ^{31}P and a ^{1}H nucleus. The angular dependence of the spectrum has been studied at 298 and 77 K. Whereas the small signal B is practically isotropic, the positions of the signals A

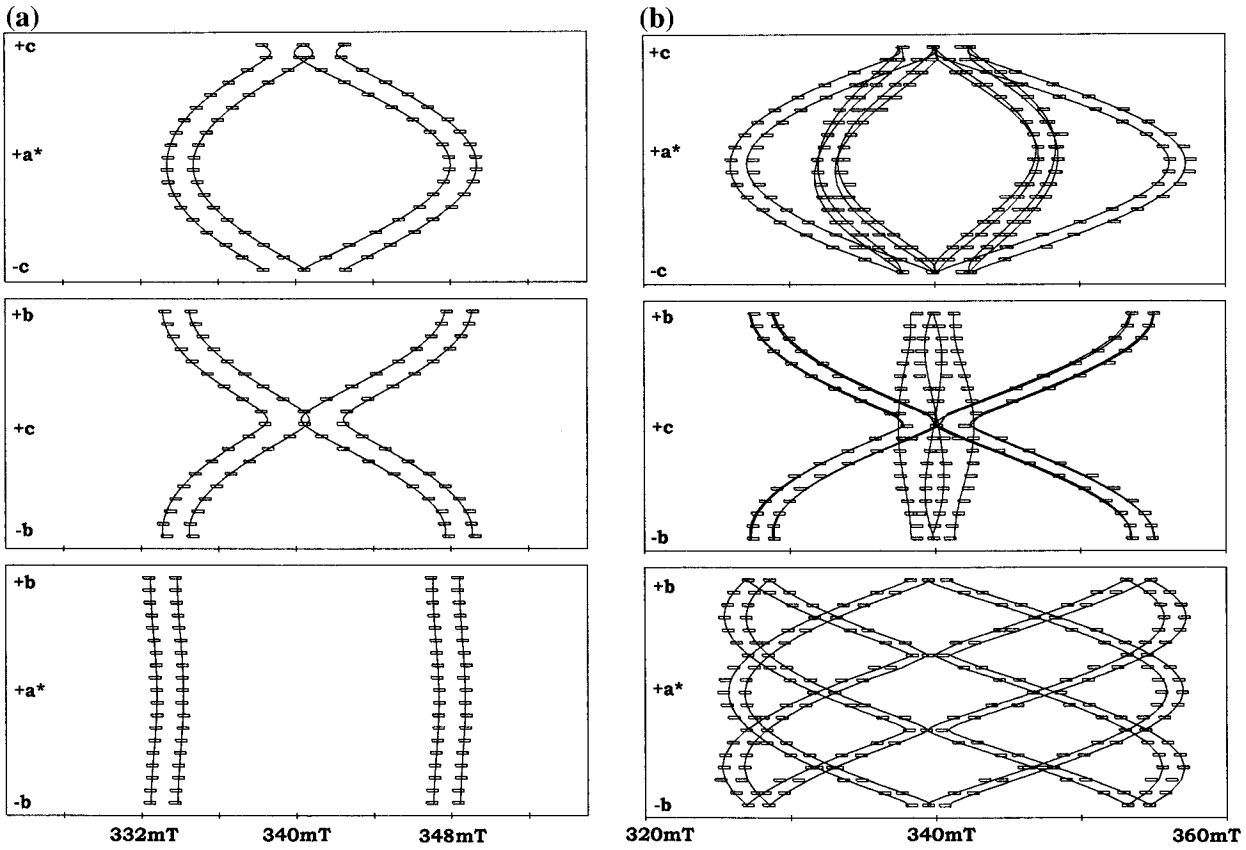

Figure 3. Angular variation of the EPR signals obtained with an X-irradiated single crystal of **2**: (a) at room temperature; (b) at 77 K.

TABLE 2: g and Hyperfine Tensors Obtained at 300 K with an X-Irradiated Single Crystal of 2

		eigenvectors		
tensor	eigenvalues[a]	**a***	**b**	**c**
g-tensor	2.0064	−0.9911	−0.0845	0.1032
	2.0082	0.0866	0.9961	0.0170
	2.0114	0.1014	−0.0246	0.9945
^{31}P-tensor (MHz)	22.6	−0.1067	0.0630	−0.9923
	409.2	0.6762	0.7363	−0.0260
	413.0	0.7290	−0.6737	−0.1212
^{1}H-tensor (MHz)	38.0	0.9097	−0.3930	−0.1342
	39.2	−0.4007	−0.9156	−0.0853
	61.3	0.1092	−0.0853	0.9903

[a] Only the absolute values of the hyperfine eigenvalues are reported in this table.

vary drastically with the orientation of the magnetic field. The resulting curves for A are shown in Figure 3; they lead to the **g** tensor and to the ^{31}P and ^{1}H hyperfine tensors that are shown in Tables 2 (room temperature) and 3 (liquid nitrogen temperature). The isotropic signal B—without any hyperfine structure—is probably due to homolytic scission of the C(8)−H(8) bond[44] and presents no interest for the present study.

Careful examination of the spectra recorded at 77 K shows that, in the region corresponding to the maximum ^{31}P splitting, an additional small line is detected on each side of the doublet A (e.g., signals A′$_1$ for the doublets A1 in Figure 2b). The separation between these lines, equal to $2g_n\beta nH$ (∼28 MHz), indicates that these signals probably correspond to forbidden spin flip transitions due to small dipolar interactions with additional protons.[12,45]

The temperature dependence of the spectrum was obtained by varying the temperature between 110 and 300 K and by recording the spectrum in steps of 10 °C. This study was performed for two orientations of the magnetic field in the *a*b* plane at 5° and 40° from the *b*-axis, respectively. The spectra obtained for some selected temperatures (former orientation) are shown in Figure 4. The line width of the three sets of doublets of doublets progressively increases between 110 and 140 K. Between 140 and 170 K the signals are so broad that they are hardly detected. Above 180 K the previous pattern is replaced by two new broad signals whose line width narrows with temperature. Above 240 K each of these lines clearly exhibits hyperfine coupling with a spin-$^1/_2$ nucleus. All these transformations were reversible. Qualitatively, these features are consistent with the trapping of the radical R(H)P$^{\bullet}$ [46,47] in three sites, which are magnetically nonequivalent at 110 K and which progressively exchange when the temperature is raised. More quantitatively, we can compare the sets of tensors obtained at 77 K with the set measured at room temperature. The eigenvalues calculated by assuming rapid jumps among the three sites—equally populated—observed at 77 K are very close to the values measured at room temperature:[51] $g_1 = 2.007$, $g_2 = 2.008$, $g_3 = 2.011$, ^{31}P $T_1 = 45$ MHz, ^{31}P $T_2 = 443$ MHz , ^{31}P $T_3 = 435$ MHz, ^{1}H $T_1 = 35$ MHz , ^{1}H $T_2 = 46$ MHz , ^{1}H $T_3 = 62$ MHz. Decomposition of these hyperfine tensors into isotropic and anisotropic coupling constants shows that the calculated ^{31}P dipolar coupling tensor and the ^{1}H A_{iso} and ^{1}H τ_{max} values[52] are in excellent agreement with the values measured at room temperature. The single discrepancy lies in the 28 MHz difference that appears between the experimental and the calculated phosphorus isotropic coupling constant. In fact this discrepancy is immediately revealed by the difference in the traces of the tensors measured at 77 K (308.6 MHz) and at room temperature (281.6 MHz). Whereas many programs have been developed to simulate the EPR spectrum resulting from the exchange between nuclei that present isotropic couplings,[8] the cases of an exchange among several sites of a system characterized by a very anisotropic hyperfine tensor are very less common. Most of the single crystal systems reported in the literature deal with the exchange between two R nuclei

TABLE 3: g and Hyperfine (MHz) Tensors Obtained at 77 K for the Three Rotameric Sites of 3 Trapped in a Single Crystal of 2

		eigenvectors								
		site 1			site 2			site 3		
tensor	eigenvalues[a]	**a***	**b**	**c**	**a***	**b**	**c**	**a***	**b**	**c**
g-tensor	2.0036	−0.9968	−0.0794	0.0031	−0.4829	0.8321	−0.2727	0.5201	0.8528	0.0482
	2.0102	−0.0033	0.0810	0.9967	−0.5635	−0.5337	−0.6306	0.4337	−0.3122	0.8452
	2.0134	0.0794	−0.9936	0.0810	−0.6703	−0.1509	0.7266	−0.7358	0.4187	−0.5322
^{31}P-tensor	4	−0.0360	0.8462	−0.5316	−0.6383	−0.3861	0.6660	−0.7124	0.4224	−0.5604
	74	−0.0416	−0.5327	−0.8453	0.5828	0.3229	0.7457	−0.4994	0.2558	0.8277
	848	−0.9985	−0.0083	0.0544	−0.5029	0.8641	0.0189	0.4930	0.8696	0.0287
^{1}H-tensor	37	0.5093	−0.7751	−0.3740	0.9942	−0.0760	−0.0785	−0.9834	−0.1658	−0.0733
	42	0.8606	0.4563	0.2264	0.0853	0.9846	0.1524	0.1724	−0.9802	−0.0971
	67	−0.0049	−0.4371	0.8994	−0.0660	0.1582	−0.9852	0.0558	0.1081	−0.9926

[a] Only the absolute values of the hyperfine eigenvalues are reported in this table.

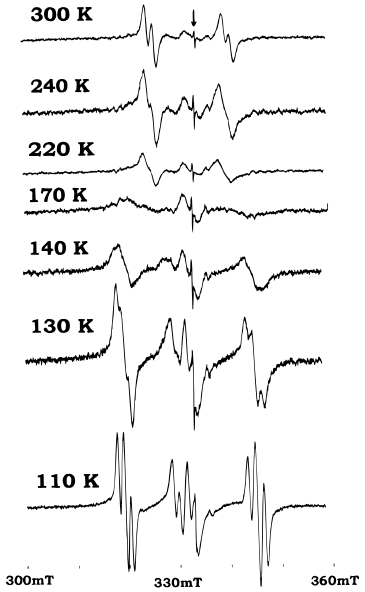

Figure 4. Temperature dependence of the EPR spectrum obtained with an X-irradiated single crystal of **2**. The magnetic field lies in the *a*b* plane, 5° from the *b*-axis. (The arrow indicates the position of the signal of DPPH.)

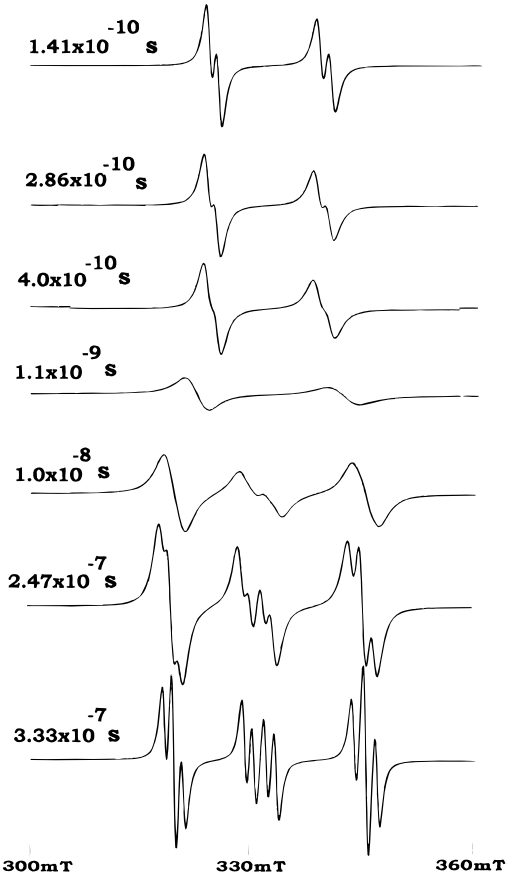

Figure 5. Simulation of the EPR spectra obtained at various temperatures with an X-irradiated single crystal of **3**. (H_o in the *a*b* plane, 5° from the *b*-axis.) The correlation time τ_c is mentioned for each spectrum. These spectra correspond to the experimental spectra shown in Figure 4 and are given in the same order.

(R = H, F) in $^{-}O(O)C-{}^{\bullet}CR_2$. In the present case, which corresponds to a three-well potential curve, we have simulated the spectra by using the density matrix theory within the Liouville formalism (see Experimental Section). In this simulation we have supposed that the three sites have the same correlation time τ_c and the same population. Between 110 and ∼160 K correlation times are found that directly lead to an excellent fitting of both the shape and the position of the experimental signals. Above 160 K the shape of the signals is perfectly simulated, but their position exhibits a shift of ∼4.5 G. This last point confirms that a slight variation in the phosphorus isotropic coupling constant (ΔA_{iso} = 28 MHz) occurs when the temperature is raised. Above 160 K the simulation was therefore performed by using an isotropic contribution to the phosphorus hyperfine interaction equal to 281 MHz. The simulations of the experimental spectra shown in Figure 4 are given in Figure 5 together with the correlation time used for the calculations.

Ab Initio Calculations. The geometry, spin densities, and the isotropic and anisotropic coupling constants were calculated after full optimization of the *tert*-butylphosphinyl radical **4**. These results are shown in Tables 4 and 5 (the *z*-axis is aligned along the C−P bond, and the *x*-axis lies in the bisector of the C(5)C(1)P and C(4)C(1)P planes). Some geometrical properties are given in Table 4. To estimate the energy barrier to the

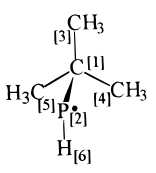

4

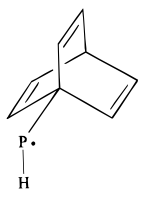

5

rotation around the C−P bond in **4,** we have optimized the structure of the radical for some selected values of the dihedral angle θ. For each conformation, the $\langle S^2 \rangle$ value was found to be equal to 0.75 after annihilation of spin contamination. The θ dependence of the energy is shown in Figure 6. The rotation barrier is equal to 2.13 kcal mol^{-1}. For **4**, we have also calculated the dipolar hyperfine interactions with additional

TABLE 4: Optimized Geometry for 4 (6-31G*, MP2)

bond lengths (Å)	bond angles (deg)	torsion angles (deg)
C(1)−P(2): 1.884	C(3)−C(1)−P(2): 109.34	C(4)−C(1)−P(2)−C(3): 120.24
C(3)−C(1): 1.538	H−P(2)−C(1): 96.26	C(5)−C(1)−P(2)−C(3): −119.92
H(6)−P(2): 1.409	C(1)−C(3)−H(7): 60.0	H(6)−P(2)−C(1)−C(4): 60.0
C(3)−H(7): 1.086		

TABLE 5: Hyperfine Coupling Constants Calculated for the Optimized Geometry of 4[a]

nucleus	isotropic coupling constant (MHz)	anisotropic coupling constants (MHz) τ_1	τ_2	τ_3
^{31}P	104	565 (0.871, 0.490, 0.001)	−276	−289
^{1}H	23	14.5 (−0.489, 0.866, −0.102)	2	−16.5

[a] The components of the eigenvectors for the maximum dipolar couplings are given in parentheses.

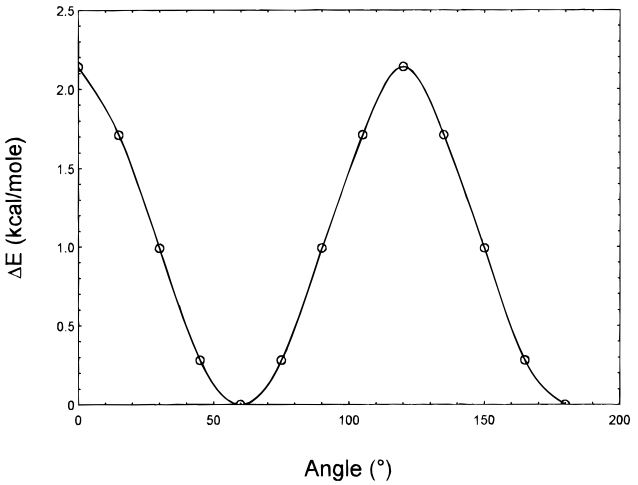

Figure 6. Variation of the energy of radical **4** as a function of the C(4)C(1)PH(6) dihedral angle.

protons H_d and $H_{d'}$, located at the positions corresponding to the benzenic hydrogen atoms H(3) and H(3′) in **3** (the coordinates of H_d and $H_{d'}$ with respect to the C(1)C(2)C(3)C(4)P fragment in $(CH_3)_3CPH$ have been obtained from the crystal structure of **2** (see Figure 1) in which the interatomic distance P···H(3) = P···H(3′) = 2.7 Å). The eigenvalues of these tensors are equal to −5, −5, and 10 MHz.

To check if the presence of three sp^2 hybridized carbon atoms in a β position to the phosphorus atom could affect the spin densities and the rotation barrier around the C−P bond, we optimized the structure of the phosphinyl radical **5** derived from the barrelenophosphine. These UHF calculations were carried out using the 3-21G* basis set. The values of $\langle S^2 \rangle$ were equal to 0.75 only for the conformations corresponding to minimum ($\theta = 60°$) and maximum ($\theta = 120°$) energies. The ^{31}P and ^{1}H isotropic couplings calculated for the optimized geometry of **5** (^{31}P-A_{iso} = 98 MHz, ^{1}H-A_{iso} = 19.4 MHz) are quite similar to those obtained for the equilibrium geometry of **4**. The rotation barrier for **5** is calculated to be equal to 1.75 kcal·mol^{-1}.

Discussion

The eigenvalues of the EPR tensors obtained at 77 K (Table 3) clearly show that the spectra A1, A2, and A3 of Figure 2b are due to the same radical. The decomposition of the hyperfine interaction into isotropic and anisotropic coupling constants—with the hypothesis of positive eigenvalues for ^{31}P T and negative eigenvalues for ^{1}H—are shown in Table 6. From a comparison with atomic coupling constants,[48] these data indicate that the unpaired electron is strongly localized in a p orbital of the phosphorus atom (73%), which is aligned along the principal component of **g** that is close to the free electron value. This is what is expected for a phosphinyl radical,[46] and additional information about the stereochemistry of the radical can be obtained by comparing the experimental coupling tensors with those calculated for **4** (Table 5). As shown by the various C(*i*)C(*j*)P bond angles and HPC(*i*)C(*j*) torsion angles, the equilibrium geometry of **4** is characterized by a tetrahedral hybridization of the central atom C(1) and by a staggered orientation of the P−H bond (H(6)PC(1)C(3) = 180°). The spin populations indicate that, as expected, the unpaired electron is mainly located (77%) in a phosphorus p orbital oriented perpendicular to the H(6)-PC(1) plane, and accordingly, the dipolar eigenvector ^{31}P-$\tau_{||}$ makes an angle of 90° with this plane. The calculated Fermi interaction with ^{31}P (104 MHz) is less than the value measured at 77 K (309 MHz) but is nevertheless quite acceptable since the difference A_{iso}(calculated) − A_{iso}(experimental) corresponds to a variation of only 0.06 in the phosphorus s character. The accord between the calculated and the experimental ^{31}P dipolar tensors is excellent. Similarly, the experimental ^{1}H Fermi contact is slightly higher than the calculated value, while the dipolar tensor well agrees with the calculated data. Both the experimental and calculated results show that the ^{1}H-τ_{max} eigenvector lies perpendicular to the ^{31}P-τ_{max} direction.

TABLE 6: Experimental Isotropic and Anisotropic Coupling Constants for 3[a]

hyperfine tensor	isotropic coupling (MHz)	anisotropic coupling (MHz) τ_1	τ_2	τ_3
^{31}P	309	−305	−235	539
^{1}H	−49	12	7	−18

[a] The ^{31}P eigenvalues have been assumed to be all positive, and the ^{1}H eigenvalues have been assumed to be negative.

More detailed information about the radical trapped at 77 K can be obtained by comparing the EPR eigenvectors with the orientation of the crystallographic bond directions. The three angles formed by the experimental ^{31}P-$\tau_{||}$ directions are equal to 120°, and each of these eigenvectors makes an angle of 90° with the crystallographic C−P direction. Moreover, as explained in the Results section, the spin flip lines observed when the magnetic field is aligned along a ^{31}P-$\tau_{||}$ direction reveal the presence of protons whose hyperfine couplings—purely dipolar—are slightly less than their nuclear Zeeman interaction. We have estimated the number of these protons by comparing the intensity of the satellite lines with that of the corresponding central line.[49] This ratio, equal to 0.055, is consistent with that for two additional protons. As mentioned above, ab initio calculations for **4** have shown that the dipolar couplings for protons located 2.7 Å from the phosphorus atom, at the position corresponding to the aromatic protons H(3) and H(3′) (Figure 7), are equal to 8 MHz when the magnetic field is aligned along ^{31}P-τ_{max}. This indicates that the spin flip lines are probably due to the proximity of these two aromatic protons. There is, therefore, no doubt that the three radical "sites" detected at 77 K correspond to the three most stable staggered conformations of the radical **3**.

From the temperature dependence of the EPR spectra it is possible to calculate the activation energy by drawing the

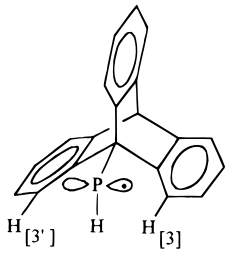

Figure 7. Position of the protons (H(3) and H(3′)) as the origin of the spin flip lines.

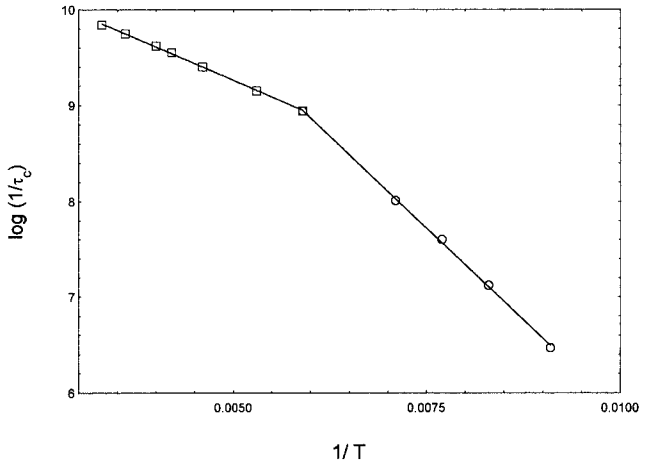

Figure 8. Variation of the correlation time τ_c with $1/T$.

Arrhenius plot $\ln(1/\tau_c) = f(1/T)$. Two straight lines are observed in the corresponding graph (Figure 8). The first one, obtained for $T < 160$ K, implies an energy activation equal to 3.5 kcal·mol^{-1} and a preexponential factor equal to 3.2×10^{12} Hz, while the second one corresponds to an activation energy of 1.6 kcal·mol^{-1} and to a preexponential factor equal to 10^{11} Hz. Although the difference between the slopes of these two lines is probably significant, we will assume that a mean value for the rotation barrier around a C−PH bond is ∼2.55 kcal·mol^{-1}. This value is in excellent agreement with the energy barrier calculated by ab initio methods for radical **4** (2.13 kcal·mol^{-1}) and for radical **5** (1.75 kcal·mol^{-1}). Our experimental value also seems reasonable when compared with data reported for diamagnetic derivatives of triptycene: for 9-hydroxytriptycene the barrier around the C−OH bond is equal to 1.28 kcal·mol^{-1}, for 9-aminotriptycene the barrier around C−NH_2 is equal to 2.56 kcal·mol^{-1}, and for 9-methyltriptycene the barrier along C−CH_3 is equal to 5 kcal·mol^{-1}.

The change in the isotropic coupling constant that occurs at 160 K is small (variation of 0.2% in the phosphorus s character) and is difficult to interpret, since for a phosphinyl radical the Fermi contact interaction arises only from inner shell polarization. We attempted to estimate the sensitivity of the ^{31}P-A_{iso} value to a distortion of the geometry of **4**; the ab initio calculations show that this constant is not very sensitive to either the CPH bond angle (1 MHz per degree) or the C−P bond distance. Moreover, when the CCPH dihedral angle is varied, the A_{iso} value is a minimum for staggered conformations and suggests that any contribution of intermediate configuration (e.g., rovibrational effect) would increase the ^{31}P-A_{iso} value. This reversible variation of the isotropic coupling perhaps reflects the presence of hydrogen bonds (e.g., interaction with the protons H(3) and H(3′) detected by the spin flip lines), which could be temperature dependent (slight expansion of the crystal cell, slight motion of the phenyl rings around their bonds with the barrelene skeleton). Such phenomenon would also explain the slight variation of the slope in the Arrhenius plot for $T >$ 160 K. It is worthwhile noticing that this small variation of the isotropic coupling would be less perceptible with a carbon-centered radical, since a variation of 0.2% in the s spin density would imply a variation of ∼7.9 MHz only.

Concluding Remarks

We have shown that direct measurement of the rotation barrier around a C−•XH bond (X = heteroatom), in the solid state, can be performed by attaching the XH_2 group to the triptycyl moiety and by studying, after irradiation, the temperature dependence of the EPR spectrum. For the C−•PH system, the experimental results are consistent (∼2.55 kcal·mol^{-1}) with the barrier of the isolated radical as expected from ab initio calculations. Nevertheless, the effects of the crystal matrix are revealed by the presence of two slopes in the Arrhenius plot.

Acknowledgment. We thank the Swiss National Science Foundation for financial support.

Supporting Information Available: Tables of atomic coordinates, isotropic and anisotropic displacement parameters, and bond lengths and angles (2 pages). Ordering information is given on any current masthead page.

References and Notes

(1) *Internal Rotation in Molecules*; Orville-Thomas, W. J., Ed.; John Wiley: London, 1974.
(2) Durig, J. R.; Gounev, T. K.; Lee, M. S.; Little, T. S. *J. Mol. Struct.* **1994**, *327*, 23−53.
(3) Janzen, E. G. In *Topics in Stereochemistry*; Allinger, N. L., Eliel, E. L., Eds.; Intersciences Publisher: New York, 1971; Vol. 6, pp 177−217.
(4) Hudson, A.; Luckhurst, G. R. *Chem. Rev.* **1969**, *69*, 191−225.
(5) Freed, J. H.; Fraenkel, G. K. *J. Chem. Phys.* **1963**, *39*, 326−348.
(6) McCalley, R. C.; Shimschick, E. J.; McConnell, H. M. *Chem. Phys. Lett.* **1972**, *13*, 115−119. Barzaghi, M.; Gamba, A; Oliva, Cesare; Branca, Mario. *Int. Rev. Phys. Chem.* **1987**, *6*, 315−336.
(7) Huang, R. H.-H.; Kivelson, D. *J. Magn. Reson.* **1974**, *14*, 202−222.
(8) Heinzer, J. *Mol. Phys.* **1971**, *22*, 167−177.
(9) Brustolon, M.; Segre, U. *J. Chim. Phys. Phys.-Chim. Biol.* **1994**, *91*, 1820−1829.
(10) Ohigashi, H.; Kurita, Y. *Bull. Chem. Soc. Jpn.* **1968**, *41*, 275−284.
(11) Sjöqvist, L.; Benetis, N. P.; Lund, A.; Maruani. J. *Chem. Phys.* **1991**, *156*, 457−464.
(12) Benetis, N. P.; Lindgren, M.; Lee, H.-S.; Lund, A. *Appl. Magn. Reson.* **1990**, *1*, 267−281.
(13) Benetis, N. P.; Mahgoub, A.; Lund, A.; Nordh, U. *Chem. Phys. Lett.* **1994**, *218*, 551−556.
(14) Peric, M.; Ravkin, B.; Dulcic, A. *Chem. Phys. Lett.* **1986**, *126*, 574−578.
(15) Benetis, N. P.; Sjöqvist, L.; Lund, A.; Maruani, J. *J. Magn. Reson.* **1991**, *95*, 523−535.
(16) Hayes, R. G.; Steible, D. J., Jr.; Tolles, W. M.; Hunt, J. W. *J. Chem. Phys.* **1970**, *53*, 4466−4469.
(17) Bogan, C. Ph.D. Thesis, The University of Alabama, 1972.
(18) Kispert, L. D.; Chang, K.; Bogan, C. M. *J. Chem. Phys.* **1973**, *77*, 629−633.
(19) Bogan, C. M.; Kispert, L. D. *J. Chem. Phys*. **1972**, *57*, 3109−3120.
(20) Kispert, L. D.; Bowman, M. K.; Norris, J. R.; Brown, M. S. *J. Chem. Phys.* **1982**, *76*, 26−30.
(21) Oki, M. *Acc. Chem. Res*. **1990**, *23*, 351−356.
(22) (a) Oki, M.; Matsusue, M.; Akinaga, T.; Matsumoto, Y.; Toyota, S. *Bull. Chem. Soc. Jpn.* **1994**, *67*, 2381−2387. (b) Nakamura, M.; Oki, M. *Bull. Chem. Chem. Soc. Jpn*. **1975**, *48*, 2106−2111.
(23) Oki, M. *Angew. Chem., Int. Ed. Engl*. **1976**, *15*, 87−93.
(24) Imashiro, F.; Hirayama, K.; Terao, T.; Saika, A. *J. Am. Chem. Soc.* **1987**, *109*, 729−733.
(25) Yamamoto, G.; Kuwahara, K.; Inoue, K. *Chem. Lett.* **1995**, 351−352.
(26) Sakakibara, K.; Allinger, N. L. *J. Org. Chem.* **1995**, *60*, 4044−4050.
(27) James, F.; Roos, M. *CERN Program Library*; CERN: Geneva, Switzerland, 1976.
(28) Iwasaki, M. *J. Magn. Reson.* **1974**, *16*, 417−423.

(29) Frisch, F. M.; Head-Gordon, M.; Trucks, G. W.; Foresman, J. B.; Schlegel, H. B.; Raghavachari, K.; Robb, M.; Binkley, J. S.; Gonzalez, C.; Defrees, D. J.; Fox, D. J.; Whiteside, R. A.; Seeger, R.; Melius, C. F.; Baker, J.; Martin, R. L.; Kahn, L. R.; Stewart, J. J. P.; Topiol, S.; Pople, J. *Gaussian 90*; Gaussian, Inc.: Pittsburgh, PA, 1990.

(30) Frisch, M. J.; Trucks, G. W.; Schlegel, H. B.; Gill, P. M. V.; Johnson, B. G.; Wong, M. W.; Foresman, J. B.; Robb, M. A.; Head-Gordon, M.; Replogle, E. S.; Gomperts, R.; Andres, J. L.; Raghavachari, K.; Binkley, J. S.; Gonzalez, C.; Martin, R. L.; Fox, D. J.; Defrees, D. J.; Baker, J.; Stewart, J. J. P.; Pople, J. *Gaussian 92/DFT*, Revision G.2; Gaussian Inc.: Pittsburgh, PA, 1992.

(31) Blanc, E.; Schwarzenbach, D.; Flack, H. D. *J. Appl. Crystallogr.* **1991**, *24*, 1035−1041.

(32) Main, P.; Fiske, S. J.; Hull, S. E.; Lessinger, L.; Germain, G.; Declercq, J.-P.; Woolfson, M. M. *A System of Computer Programs for the Automatic Solution of Crystal structures from* X-*R*ay *Diffraction Data;* University of York and Louvain-la-Neuve: England and Belgium, 1987.

(33) Hall, S. R., Flack, H. D., Stewart, J. M., Eds. *XTAL3.2 User's Manual*; Universities of Western Australia and Maryland: Nedlands, Australia and College Park, MD, 1992.

(34) Johnson, C. K. ORTEP II. Report ORNL-5138; Oak Ridge National Laboratory: Oak Ridge, TN, 1976.

(35) *International Tables for X-ray Crystallography*; Kynoch Press: Birmingham, England, 1974.

(36) Flack, H. D. *Acta Crystallogr*. **1983,** *A39*, 876−881.

(37) Bernardinelli, G.; Flack, H. D. *Acta Crystallogr.* **1985**, *A41*, 500−511.

(38) Le Page, Y. *J. Appl. Crystallogr.* **1987**, *20*, 264−269.

(39) Tabushi, I.; Yoshida, Z.; Aoyama, Y. *Bull. Chem. Soc. Jpn*. **1974**, *47*, 3079−3083.

(40) Freijee, F. J. M.; Stam, C. H. *Acta Crystallogr*. **1980**, *B36*, 1247−1249.

(41) Van der Putten, N.; Stam, C. H. *Acta Crystallogr*. **1980**, *B36*, 1250−1252.

(42) Smit, F.; Stam, C. H. *Acta Crystallogr*. **1980**, *B36*, 1254−1256.

(43) Schomburg, D.; Sheldrick, W. S. *Acta Crystallogr*. **1975**, *B31*, 2427−2431.

(44) Reichel, C. L.; McBride, J. M. *J. Am. Chem. Soc*. **1977**, *99*, 6758−6760.

(45) Geoffroy, M.; Ginet, L.; Lucken, E. A. *Mol. Phys.* **1976**, *31*, 745−754.

(46) Geoffroy, M.; Lucken, E. A. C.; Mazeline, C. *Mol. Phys.* **1974**, *28*, 839−845.

(47) Tordo, P. In *The Chemistry of Organophosphorus Compounds*; Patai, P., Hartley, F., Eds.; J. Wiley: New York, 1990; Vol. 1, p 437.

(48) Morton, J. R.; Preston, K. F. *J. Magn. Reson.* **1978**, *30*, 577−582.

(49) (a) Bowman, M.; Kevan, L.; Schwartz, R. N. *Chem. Phys. Lett.* **1975**, *30*, 208−211. (b) Schlick, S; Kevan, L. *J. Magn. Reson.* **1976**, *22*, 171−181. (c) Schlick, S.; Kevan, L. *J. Magn. Reson.* **1976**, *21*, 129−133.

(50) 9-Phosphinotriptycene is the trivial name for 9-phosphino-10-hydrobenz[1′,2′]anthracene. The molecular structure in the solid state (vide infra) being symmetric (C_3), it was judicious to renumber the atoms taking into account the asymmetric unit. This numbering is shown in Figure 1.

(51) In this calculation the three tensors expressed in the experimental reference frame are added, and the resulting tensor is divided by three and diagonalized.

(52) The experimental proton dipolar tensor exhibits an axial symmetry that is more pronounced than for the calculated tensor. This probably reflects a modest precision on the measurement of the proton splittings, at 77K, due to an overlap of two sites in the planes *a***c* and *bc*.

JP960836H